ARTICLE

Terahertz time domain spectroscopy of graphene and MXene polymer composites

Klaudia Zeranska-Chudek[1] [ID] | Anna Lapinska[1] | Agnieszka Siemion[1] |
Agnieszka M. Jastrzębska[2] | Mariusz Zdrojek[1]

[1]Faculty of Physics, Warsaw University of Technology, Warsaw, Poland

[2]Faculty of Materials Science and Engineering, Warsaw University of Technology, Warsaw, Poland

Correspondence
Klaudia Zeranska-Chudek, Faculty of Physics, Warsaw University of Technology, Koszykowa 75, 00-662 Warsaw, Poland.
Email: klaudia.zeranska@pw.edu.pl

Abstract

The rising demand for faster and more efficient electronic devices forces electronics industry to shift toward terahertz frequencies. Therefore there is a growing need for efficient, lightweight, and easy to produce absorbing materials in the terahertz range for electromagnetic interference (EMI) shielding and related applications. This study presents a study on basic optical properties of two types polymer-based composites loaded with two-dimensional structures—graphene and MXene phases (Ti_2C). In said range, total EMI shielding efficiency (SE) and its components, the absorption coefficient (α), refractive index, and complex dielectric function are investigated. The ratio of SE absorption component to reflection component (SE_{ABS}:SE_R) of fabricated composites is equal or higher than 30:1 in over 80% of studied range. The fabricated composites exhibit low (<0.1) loss tangent in studied range. The addition of 1 wt% of graphene increases the composite α over 10-fold in respect to pure polymer–up to 60 cm^{-1} for frequency higher than 2 THz.

KEYWORDS

optical and photovoltaic applications, optical properties, packaging, spectroscopy

1 | INTRODUCTION

In pursuit of higher performance, the electronics industry has been showing more and more interest in electronic devices working in the terahertz range (0.1 – 10 THz), in various sectors, that is, astronomy, biomedical imaging, and security.[1–4] Growing number of devices working, and thus emitting stray radiation at the terahertz range, contributes to the growth of electromagnetic (EM) pollution in said range. On the other hand, the development of various terahertz techniques requires new innovative materials for optical applications, that is, passive absorbing elements or saturable absorbers operating in the terahertz range. Therefore there is a high and persistent need for novel lossy materials and a thorough study regarding their complex optical properties in the THz range.

Proper shielding of electronic devices from stray EM radiation is a complex but important task. Stray EM radiation produced by standard operation of electronic devices, such as communication antennas, mobile phones or personal computers, leads to electromagnetic interference, which may influence the operation of delicate electronic devices resulting in malfunctions, data leakage in digital communication or if medical equipment is affected, even pose danger to human health.[5] The choice of proper lossy material during an electronic device design is vital, as neither "overshielding" nor "undershielding" of the device is wanted.[6] Undershielding enables the radiation to penetrate the device packaging and thus provokes malfunction of said devices, while overshielding often results in added production costs and excess weight. That is why novel lightweight materials,

based on polymer matrixes loaded with conductive particles, especially those based on two-dimensional (2D) materials, are being developed to replace commonly used metals. The polymer-based materials can provide sufficient EM interference shielding effectiveness (EMI SE; >30 dB, which corresponds to shielding of 99.9% of the incident radiation) and low penetration depth of EM waves (high absorption coefficient >40 cm^{-1}) at low weight.[7–9] What is more, polymer composites with 2D materials inclusions are easy to fabricate, not prone to corrosion and their electrical, thermal, and mechanical properties can be tuned to fit the desired application, as opposed to the conventional metal-based or metal particles infused polymer composite shields.

Another argument against commonly used metallic shields is that they exhibit mostly electrically induced reflection shielding mechanisms (the radiation is scattered on the free carriers). Reflection-based shielding mechanism only redirects the stray radiation. To tackle the EM pollution, a material capable of radiation absorption rather than reflection is needed. We have already reported a nonconductive polymer-based material exhibiting good shielding efficiency based on absorption mechanism in one of our previously published works.[10] However, the studied materials were examined in a narrower frequency range and no other optical properties than shielding efficiency were studied.

While shielding efficiency and its components are crucial factors for EMI shielding applications, it is also vital to examine other optical properties of potential lossy materials, like the absorption coefficient, loss tangent, or the refractive index. These optical properties may determine possible applications of the material, for example, waveguide absorbing loads or passive optical elements. Only the full information on optical and dielectric properties can give exhausting insight on the material.

The literature provides many examples of polymer-based composites loaded with nanofillers for EMI shielding applications. Composites and foams employing both MXene and graphene nanofillers that exhibit high SE values have already been reported,[11–13] but the studied frequency range is usually restricted to the X-band. Zhang et al. have reported a graphene foam of high shielding efficiency in a broad range of microwave frequencies. They have also investigated the dielectric properties of the material,[14] but no information was provided on its basic optical properties, like transmittance and reflectance, which can provide information on the main shielding mechanism of the material. The terahertz range brings new opportunities for novel devices based on graphene or MXenes. For example, Khromova et al. have reported a graphene-based terahertz/infrared waveguide modulator,[15] another study shows a MXene-based terahertz detector.[16] Although there are some works on graphene, or MXene-based composites utilized as terahertz radiation shields,[17,18] to our best knowledge, none of these studies show a comparison of shielding and optical properties of series of composites containing different nanofillers fabricated with the same production method and nanofiller loading. We find such a work could be beneficial to the general state of knowledge and would provide insight on the influence of different nanofillers on the same matrix, under specified conditions, and as such, could be a road mark for future studies.

In this work we provide an extensive comparative study on the optical and dielectric properties of polymer composites infused with two types of nanoparticles via terahertz time domain spectroscopy. Time domain spectroscopy in the THz regime (THz-TDS) is a technique that allows a facile determination of not only the transmittance and reflectance and thus total shielding effectiveness and its components, but also the absorption coefficient, dielectric permittivity (also referred to as dielectric constant), loss tangent, and refractive index of the measured material. The shielding performance and other basic optical properties of the fabricated composites vary, depending on the nanofiller employed in the composite. We report two series of polymer-based shielding materials exhibiting absorption-based shielding mechanism. Samples containing graphene nanoplatelets show most notable differences in measured properties from pristine polymer, exhibiting total SE of 40 dB and absorption coefficient higher than 60 cm^{-1} (for frequencies above 1.7 THz). We report low loss tangent of fabricated composites (0.64 maximum value for graphene composite) and refractive index values between 1.6 and 2, similar to those of pristine polymer. Finally, we report a series of elastic, nonconductive, low-dielectric loss, and low-reflection polymer composites with poor to high EMI shielding efficiency, depending on the 2D filler used, and absorption as the main shielding mechanism.

2 | METHODS AND MATERIALS

2.1 | Sample fabrication

Graphene flakes (5-μm lateral flake size) were supplied by Sigma Aldrich and MXene particles (Ti$_2$C) were supplied by a group at Faculty of Material Science, Warsaw University of Technology. Production of MXene particles has been described in our previous studies.[19] All 2D materials were fabricated or purchased in the form of powder. Polydimethylsiloxane (PDMS) was purchased from Dow Corning Co., as a two-part liquid component kit, containing base and curing agent (Sylgard 184).

PDMS composites were fabricated using a simple blend mixing method. A specific weight of 2D materials (depending on the desired loading in the composite) was added to the PDMS base solution. To distribute the particles in the polymer precursor, the mixture was placed in an ultrasonic bath (Elmasonic) for 2–3 h and afterward stirred on a magnetic stirrer for 1 h. Then the curing agent was added to the mixture in 10:1 (PDMS base + 2D material: PDMS curing agent) proportions. The mixture was then degassed to remove any bubbles created in the fabrication process. Finally, the mixture was cured at high temperature (100 °C) for one hour. The amount of 2D materials was calculated to meet the loading of 1 wt% in all composites. The specific nanofiller loading was chosen based on our previous works on PDMS composites containing graphene inclusions, where we showed the influence of graphene loading on optical properties of fabricated composites.[10,20] For reference, a sample containing no additives was also fabricated. All composites were fabricated in the form of a flat flexible slab 700 μm ± 20% thick (see Figure 1(b)). From now on, the composites will be referred to by the nanofiller type used during the fabrication.

2.2 | Sample characterization

THz-TDS measurements were conducted using TeraView spectrometer Spectra 3000. The system is based on an 800 nm femtosecond laser generating 50 fs pulses. The spectrometer can provide data in $0.06 - 4$ THz ($2 - 120$ cm^{-1}) range with 0.0075 Hz (0.25 cm^{-1}) resolution. The measurements were taken in a Rapid Scan mode – 30 scans per second with 1.25 cm^{-1} resolution. Measurements were conducted in ambient temperature. Before measurements, the thickness of each sample had been checked and a series of scans had been conducted for each type of composite. The TeraView software was used to retrieve the refractive index, absorption coefficient, transmittance, reflectance, and the complex dielectric function of the measured composites. For more straightforward data analysis, we have normalized the data to represent the features of a 500-μm thick sample.

We have collected Raman spectra of all fabricated samples, the data are shown in Figure 1(c). One can see, that the peaks characteristic for PDMS are repeated in every composite spectrum, but for composites we can observe the signature peaks for every 2D additive—for graphene: 1353, 1576, and 2702 cm^{-1} (D, G, and 2D[21]); for Ti$_2$C: 1397 and 1573 cm^{-1} (also D and G[22]).

For the Fourier transform infrared (FTIR) measurements, a Bruker VERTEX 80v spectrometer was used. The FTIR transmittance spectra presented in Figure 1(d) show direct influence of filler presence and filler type on the optical properties of the fabricated composites. While the pure PDMS sample shows highest transmittance level of ~90%, the MXene composite transmits only ~20% of incident radiation and graphene sample shows no
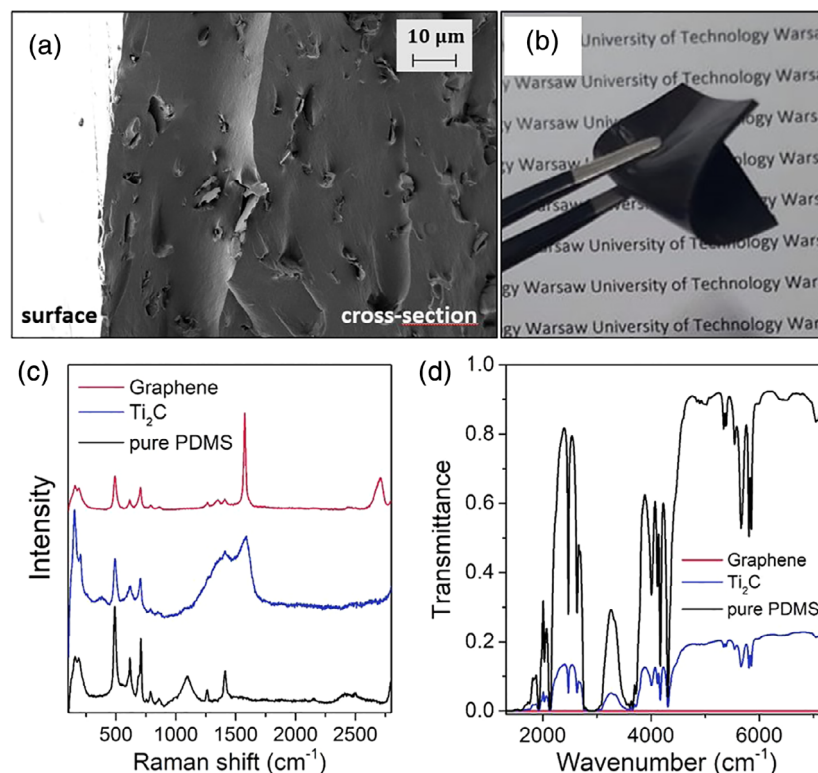

FIGURE 1 PDMS composites (a) a SEM image of a cross-section of the graphene/PDMS composite, (b) an image showing the flexibility of the graphene/PDMS composite, and (c) Raman spectra of the fabricated composites. (d) FTIR transmittance spectra of fabricated composites. FTIR, Fourier transform infrared; PDMS, polydimethylsiloxane [Color figure can be viewed at wileyonlinelibrary.com]

transmittance at all. Graphene and MXene composites show no characteristic features except for those characteristic to pure PDMS. The PDMS/graphene composites' FTIR spectra are in good agreement with our previous work, where we have studied composites of different (0.02–2 wt%) graphene loading.[20]

Sheet resistance of the fabricated composites was measured using a four-point probe method. The DC resistivity measurements showed no difference between composites and pure polymer, regardless of the nanofiller. Also the scanning electron microscope (SEM) image (see Figure 1(a)) shows small aggregates of nanoparticles, but no visible percolation paths. Based on that we state our composites are completely nonconductive in DC.

3 | RESULTS AND DISCUSSION

Figure 2 shows collected transmittance and reflectance spectra of fabricated composites. As seen in Figure 2(a), the transmittance of composites is lower than the transmittance of pure PDMS. The composite containing graphene nanoplatelets shows a significant decrease of the transmittance, a small decrease is also visible in the
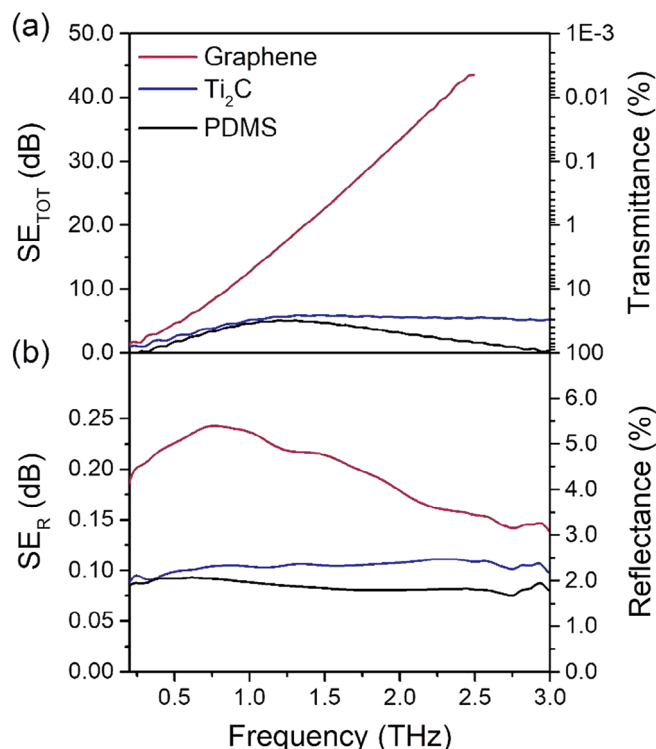

FIGURE 2 Basic optical properties of fabricated composites in THz regime. (a) Measured transmittance and calculated total shielding effectiveness SE_{TOT}. (b) Measured reflectance and calculated reflection component of shielding efficiency SE_R [Color figure can be viewed at wileyonlinelibrary.com]

Ti$_2$C composite. Regardless of the nanofiller, transmittance is decreasing with growing frequencies up to ~1.2 THz. For higher frequencies, transmittance of Ti$_2$C composite is reaching a plateau (at ~30%). The graphene composite shows a constant decrease in transmittance with the growing frequency up to ~2.5 THz, for higher frequencies the data is no longer reliable.

The reflectance spectra (see Figure 2(b)) show a relatively low level of reflectance (1.5–5.5%) in the whole studied frequencies range. There is no specific trend in the spectra with respect to the different nanofillers used. Low reflectance seems to be determined by the PDMS signature, again only the graphene composite shows any significant difference from the pristine polymer.

Using the transmittance and reflectance data, the total shielding efficiency (SE_{TOT}) and its reflectance component (SE_R) were calculated. It is known that the shielding efficiency of a material is calculated as $SE = -10\log_{10}(T)$, where T represents the transmittance of studied material. Shielding efficiency is comprised of three components—the reflection (SE_R), absorption (SE_{ABS}), and multiple inner reflection (SE_{MIR}) components. The total shielding effectiveness can be calculated as a sum of its components $SE_{TOT} = SE_R + SE_{ABS} + SE_{MIR}$. Due to the fact that incident wavelength is longer than the thickness of the composite, multiple inner reflection component can be omitted. The remaining reflection and absorption components can be calculated as $SE_R = -10\log_{10}(1 - R)$ and $SE_{ABS} = -10\log_{10}\left(\frac{T}{1-R}\right)$, respectively, R being the measured reflectance. Calculating the components of shielding effectiveness can determine the main shielding mechanism of the studied material. In case of fabricated composites, the reflection component is relatively small compared to the total shielding effectiveness, regardless of the nanofiller used. Reflection component has a maximum of 5% share in the total shielding effectiveness in at least 0.87 of studied range in case of graphene composites and even up to 0.93 of the studied range for samples loaded with MXene nanoplatelets. This implies that the absorption component, being the difference of the total shielding effectiveness and its reflection component, seems to be the dominating shielding mechanism. Graphene composite exceeds the shielding efficiency value of 40 dB for frequencies higher than ~2.2 THz, while the other composite remains below 10 dB in the whole studied range. SE of graphene composite is suitable for most shielding applications in the terahertz range,[6] MXene composite can be utilized in applications requiring less effective shielding and small reflectance, for example, waveguide loads and terminations, or cavity resonance reduction.[23,24]

The refractive index of fabricated composites, shown in Figure 3(a) is nearly featureless in the terahertz range, which is consistent with the literature.[18,25,26] The ~1.6 value of pure PDMS sample is similar to that measured by Kim et al.[25] It should be noted that thin films made of corresponding 2D materials typically show relatively higher refractive indices than those of composite materials.[27,28] However, the graphene composite and graphene dispersion reported by other groups show similar (<2) refractive index,[18,26] which suggests the composites owe the low value of the refractive index to the polymer matrix, with nanofillers only slightly influencing the resulting value.

The dependence of dielectric constants or dielectric permittivity (both real ϵ' and imaginary ϵ'') and the corresponding loss tangent ($\tan \delta$) on frequency is shown in Figure 3(b,c). All composites show low values of both dielectric permittivity and the loss tangent, compared to other state of the art composites and suspensions.[29] There is a visible difference between graphene and other composites, both in values and shape of the dielectric properties spectra. Graphene composite samples show ϵ', ϵ'', and $\tan\delta$ values of approximately 3.4, 0.22, and 0.064 respectively at the frequency of 1.5 THz. These values exceeded those of pristine polymer by 1.4 to 5 times, depending on the property. In contrast to other fabricated composites, the ϵ'' and $\tan\delta$ of the graphene composite are growing with the rising frequencies up to 2.2 THz, where it reaches a maximum value. The dielectric properties of composite with MXene nanofillers show a vague decrease with the growing frequencies (the ϵ' reaching a plateau at ~1.5 THz) and are similar to those of pristine polymer. The Ti$_2$C composite shows 30% increment in loss tangent at 1.5 THz in respect to the pristine

polymer. Overall low values of loss tangent and the real part of dielectric permittivity may indicate low dielectric absorption in studied material.

Figure 4 shows the absorption coefficient of fabricated composites. Again, composite containing graphene shows the biggest deviation from pure polymer. The absorption coefficient of graphene/PDMS composite shows visible growth tendency ranging from ~10 cm^{-1} at 0.5 THz to >60 cm^{-1} at 2.2 THz which is over 10 times higher than the absorption coefficient of a pure polymer at the same frequency. The absorption coefficient of Ti2C enriched
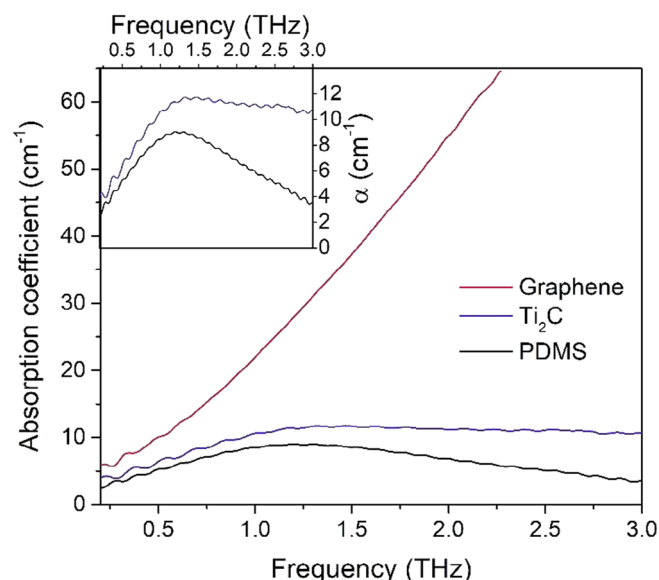

FIGURE 4 Absorption coefficient of the PDMS composites with an inset graph for composites with low absorption coefficient. PDMS, polydimethylsiloxane [Color figure can be viewed at wileyonlinelibrary.com]
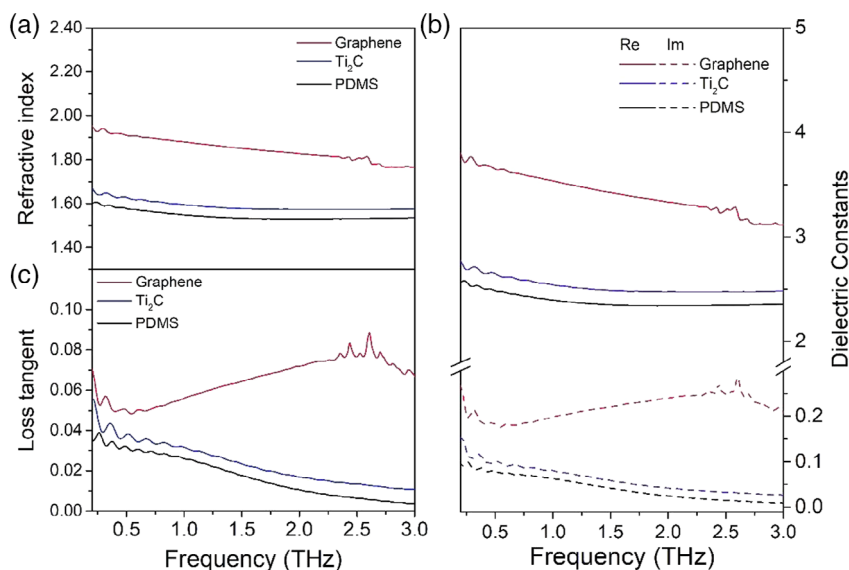

FIGURE 3 (a) Refractive index, (b) dielectric constants, and (c) loss tangent of the fabricated composites [Color figure can be viewed at wileyonlinelibrary.com]

TABLE 1 Comparison with previously reported absorption coefficients of studied nanomaterials or polymer composites with nanomaterial additives

Material	α (cm^{-1}) @ 1 THz	α (cm^{-1}) @ 1.5 THz	α (cm^{-1}) @ 2 THz
Pure PDMS[30]	10.2	11.1	10.1
Graphene/PET–DLA composite[18]	23.5	57.4	-
Graphite/PE composite[31]	25.6	48.3	83.0
Graphene oxide/PE composite[31]	2.2	3.7	6.4
Reduced graphene oxide/PE composite[31]	13.5	14.9	19.5
Ti$_3$C$_2$ thin film[27]	57.7	43.9	32.9
Graphene/PDMS composite	**21.9**	**37.2**	**54.9**
Ti$_2$C/PDMS composite	**10.6**	**11.7**	**11.2**
Pure PDMS	**8.5**	**8.5**	**6.9**

Note: Materials studied in this paper are in bold.
Abbreviations: DLA, di-linoleic acid; PDMS, polydimethylsiloxane; PE, polyethylene; PET, polyethylene terephthalate.

composite shows a slight growth tendency up to 1.2 THz, where it reaches ~11 cm^{-1} and remains stable up to 3 THz.

For reference, we show a comparison of absorption coefficients characteristic for composites and thin films based on graphene and MXenes (see Table 1), found in literature. What is interesting, the absorption coefficient of MXene composite is much lower than that of a Ti3C2 MXene thin film.[27]

Regarding polymer composites with carbon-based fillers reported so far, there is variation of absorption coefficient depending on the specific filler type, as seen in Table 1. Koroliov group has recently reported on a similar polymer composite (a copolyester matrix of polyethylene terephthalate [PET] and di-linoleic acid [DLA]) with graphene nanoplatelets.[18] Although the values of absorption coefficient are slightly higher for the PET–DLA composite (such value may be influenced by polymer matrix absorption coefficient that has not been reported in that work), the shape of the spectrum corresponds to the one we have shown in this work. Also the absorption coefficient we have observed for graphene composite exhibits a growth that can be related to an absorption band characteristic for carbon materials in polymer matrixes at 2.2 THz.[31] We assume the shape of absorption coefficient spectra is associated with the relation between graphene flake size (diameter ϕ) and the wavelength of the incident radiation (λ). Given the average graphene flake diameter as ~5 μm (as stated by the supplier and as seen in Figure 1

(a)) and the wavelength of ~100 – 3000 μm, we can state that $\phi \ll \lambda$, and so our material follows a model described by Chamorro-Posada et al.,[31] which describes EM waves interaction with system of conductive centers (graphene or MXene flakes) in a polymer matrix. However, the aforementioned model has been analyzed in reference to sp^2 carbon materials and cannot be expanded to MXene samples. Chamorro-Posada et al. state that the rapid growth of absorption near 2.2 THz frequency is largely contributed to by specific inter-planar vibrations in sp^2 carbons. They also suggest stacking high numbers of carbon layers enhances the absorption, which could explain high SE and absorption coefficient in our graphene flakes-based composite samples. What is more, following the work by Bychanok et al.,[32] the geometry of graphene flakes used in this study is highly beneficial for the absorption properties of the composite, as they exhibit high aspect ratio (surface to thickness ratio).

The results obtained for pure PDMS sample are consistent with the literature values to the order of magnitude,[30,33] which does not match the resolution of the measurement. The absorption coefficient of PDMS is highly dependent on the fabrication process of the polymer, especially the curing temperature. As Salman et al. reports, a change from 60 to 120°C can alter the absorption coefficient from ~9.6 to ~20.3 cm^{-1} at 1 THz frequency.[33] The absorption coefficient of our PDMS polymer samples is clearly lower than the values reported by Salman et al. That difference may stem in shorter curing time – 1 h on our part and 6 h in case of the literature data. Shorter curing time may have not stimulated the level of cross-linking within the polymer responsible for ameliorating the absorption coefficient.[33]

4 | CONCLUSIONS

We have successfully utilized THz time-domain spectroscopy to perform a thorough comparative study of optical properties of polymer composites enhanced with 2D materials in range of 0.2–3 THz. We have prepared three types of PDMS composites with various 2D materials—graphene and Ti$_2$C at 1 wt% loading, fabricated using a simple blending method. We have shown the shielding effectiveness and its main components (calculated using transmittance and reflectance data), refractive index, loss tangent, the complex dielectric function and absorption coefficient of said composites. The shielding effectiveness ranges from highly shielding –40 dB graphene composite, through somewhat shielding (~6 dB) MXene composite, to low SE of pristine polymer. The MXene show surprisingly low SE when employed in a polymer composite, especially taking into account the SE of a MXene thin

film. Nevertheless all composites show absorption as main shielding mechanism with very low reflectance – <5% in the whole studied range. All composites show low dielectric loss with small deviations for graphene composites. Refractive index of all composites is similar to that of pure polymer.

CONFLICT OF INTEREST
The authors declare no potential conflict of interest.

ORCID
Klaudia Zeranska-Chudek https://orcid.org/0000-0001-8677-4100

REFERENCES
[1] T. Nagatsuma, G. Ducournau, C. C. Renaud, *Nat. Photonics* **2016**, *10*, 371.
[2] Y. Kawano, in *Handbook of Terahertz Technology for Imaging, Sensing and Communications* (Ed. D. Saeedkia), Woodhead Publishing Series in Electronic and Optical Materials, Woodhead Publishing, Cambridge, UK, **2013**, pp. 403–422.
[3] D. Saeedkia, in *Handbook of Terahertz Technology for Imaging, Sensing and Communications* (Ed. D. Saeedkia), Woodhead Publishing Series in Electronic and Optical Materials, Woodhead Publishing, Cambridge, UK, **2013**, pp. 3–27.
[4] X. Wu, H. Lu, K. Sengupta, *Nat. Commun.* **2019**, *10*, 2722.
[5] R. S. Ferguson and T. Williams, in *Telecommunications Engineer's Reference Book* (Ed. F. Mazda), Butterworth-Heinemann, Oxford, UK, **1993**, pp. 23–1.
[6] D. Markham, *Mater. Des.* **1999**, *21*, 45.
[7] Z. Zeng, H. Jin, M. Chen, W. Li, L. Zhou, Z. Zhang, *Adv. Funct. Mater.* **2016**, *26*, 303.
[8] Y. Chen, H.-B. Zhang, Y. Yang, M. Wang, A. Cao, Z.-Z. Yu, *Adv. Funct. Mater.* **2016**, *26*, 447.
[9] H. John, R. M. Thomas, J. Jacob, K. T. Mathew, R. Joseph, *Polym. Compos.* **2007**, *28*, 588.
[10] M. Zdrojek, J. Bomba, A. Łapińska, A. Dużyńska, K. Żerańska-Chudek, J. Suszek, L. Stobiński, A. Taube, M. Sypek, J. Judek, *Nanoscale* **2018**, *10*, 13426.
[11] Y. Chen, Y. Wang, H.-B. Zhang, X. Li, C.-X. Gui, Z.-Z. Yu, *Carbon* **2015**, *82*, 67.
[12] K. Raagulan, R. Braveenth, H. J. Jang, Y. Seon Lee, C.-M. Yang, B. Mi Kim, J. J. Moon, K. Y. Chai, *Materials* **2018**, *11*, 1803.
[13] R. Sun, H.-B. Zhang, J. Liu, X. Xie, R. Yang, Y. Li, S. Hong, Z.-Z. Yu, *Adv. Funct. Mater.* **2017**, *27*, 1702807.
[14] Y. Zhang, Y. Huang, T. Zhang, H. Chang, P. Xiao, H. Chen, Z. Huang, Y. Chen, *Adv. Mater.* **2015**, *27*, 2049.
[15] I. Khromova, A. Andryieuski, A. Lavrinenko, *Laser Photonics Rev.* **2014**, *8*, 916.
[16] Y. I. Jhon, M. Seo, Y. M. Jhon, *Nanoscale* **2017**, *10*, 69.
[17] S.-T. Xu, F. Fan, J. Cheng, H. Chen, W. Ma, Y. Huang, S. Chang, *Adv. Optic. Mater.* **2019**, *0*, 1900555.
[18] A. Koroliov, G. Chen, K. M. Goodfellow, A. N. Vamivakas, Z. Staniszewski, P. Sobolewski, M. E. Fray, A. Łaszcz, A. Czerwinski, C. P. Richter, R. Sobolewski, *Appl. Sci.* **2019**, *9*, 391.
[19] A. Szuplewska, D. Kulpińska, A. Dybko, A. M. Jastrzębska, T. Wojciechowski, A. Rozmysłowska, M. Chudy, I. Grabowska-Jadach, W. Ziemkowska, Z. Brzózka, A. Olszyna, *Mater. Sci. Eng., C* **2019**, *98*, 874.
[20] K. Zeranska-Chudek, A. Lapinska, A. Wroblewska, J. Judek, A. Duzynska, M. Pawlowski, A. M. Witowski, M. Zdrojek, *Sci. Rep.* **2018**, *8*, 9132.
[21] A. C. Ferrari, J. C. Meyer, V. Scardaci, C. Casiraghi, M. Lazzeri, F. Mauri, S. Piscanec, D. Jiang, K. S. Novoselov, S. Roth, A. K. Geim, *Phys. Rev. Lett.* **2006**, *97*, 187401.
[22] F. Liu, A. Zhou, J. Chen, H. Zhang, J. Cao, L. Wang, Q. Hu, *Adsorption* **2016**, *22*, 915.
[23] Y. Luo, Z. Liang, D. Meng, J. Tao, J. Liang, C. Chen, J. Lai, Y. Qin, J. Lv, Y. Zhang, *Opt. Commun.* **2019**, *448*, 1.
[24] Y. Arbaoui, V. Laur, A. Maalouf, P. Quéffélec, D. Passerieux, A. Delias, P. Blondy, *IEEE Trans. Microw. Theory Tech.* **2016**, *64*, 271.
[25] D.-S. Kim, D.-H. Kim, S. Hwang, J.-H. Jang, *Opt. Express* **2012**, *20*, 13566.
[26] S. Skalsky, J. Molloy, M. Naftaly, T. Sainsbury, K. R. Paton, *Nanotechnology* **2018**, *30*, 025709.
[27] G. Choi, F. Shahzad, Y.-M. Bahk, Y. M. Jhon, H. Park, M. Alhabeb, B. Anasori, D.-S. Kim, C. M. Koo, Y. Gogotsi, M. Seo, *Adv. Optic. Mater.* **2018**, *6*, 1701076.
[28] J. T. Hong, K. M. Lee, B. H. Son, S. J. Park, D. J. Park, J.-Y. Park, S. Lee, Y. H. Ahn, *Opt. Express* **2013**, *21*, 7633.
[29] F. Marra, A. G. D'Aloia, A. Tamburrano, I. M. Ochando, G. De Bellis, G. Ellis, M. S. Sarto, *Polymer* **2016**, *8*, 272.
[30] S. Alfihed, M. H. Bergen, A. Ciocoiu, J. F. Holzman, I. G. Foulds, *Micromachines* **2018**, *9*, 453.
[31] P. Chamorro-Posada, J. Vázquez-Cabo, Ó. Rubiños-López, J. Martín-Gil, S. Hernández-Navarro, P. Martín-Ramos, F. M. Sánchez-Arévalo, A. V. Tamashausky, C. Merino-Sánchez, R. C. Dante, *Carbon* **2016**, *98*, 484.
[32] D. Bychanok, P. Angelova, A. Paddubskaya, D. Meisak, L. Shashkova, M. Demidenko, A. Plyushch, E. Ivanov, R. Krastev, R. Kotsilkova, F. Y. Ogrin, P. Kuzhir, *J. Phys. D Appl. Phys.* **2018**, *51*, 145307.
[33] S. Alfihed, M. H. Bergen, J. F. Holzman, I. G. Foulds, *Polymer* **2018**, *153*, 325.